

A Periodic Mixed Linear State Space Model to Monthly Long-term Temperature Data

M. Costa¹ & M. Monteiro

ESTGA - Águeda School of Technology and Management, University of Aveiro, Portugal

CIDMA - Center for Research & Development in Mathematics and Applications, University of Aveiro,
Portugal

Abstract

In recent decades, the world has been confronted with the consequences of global warming; however, this phenomenon is not reflected equally in every part of the globe. Thus, the warming phenomenon must be monitored in a more regional or local scale. This paper analyzes monthly long-term time series of air temperatures in three Portuguese cities: Lisbon, Oporto and Coimbra. We propose a periodic state space framework, associated with a suitable version of the Kalman filter; which allows for the estimation of monthly warming rates taking into account the seasonal behavior and serial correlation. Results about the monthly mean of the daily mid-range temperature time series show that there are different monthly warming rates. The greatest annual mean rise was found in Oporto with 2.17°C whereas, in Lisbon and Coimbra, it was respectively, 0.62°C and 0.55°C , per century.

¹Corresponding author: M. Costa, ESTGA & CIDMA, Universidade de Aveiro, Apartado 473, 3754-909 Águeda, Portugal, Email: marco@ua.pt

18 Keywords: Air temperature, Climate change, Kalman filter, Portuguese cities, Seasonality, Time series
19 analysis

20 **1 Introduction**

21 The rise in global temperature has been of increasing concern for several authorities. Accordingly to the
22 Intergovernmental Panel on Climate Change, the world's greenhouse gas emissions are continuing increasing
23 and on the current scenario, global temperature rise will far exceed the limit goal of 2°C that countries have
24 agreed with in order to avoid the most dangerous impacts on climate change. In the United Nations (UN)
25 Framework, countries adopted the Paris Agreement, on 12 December 2015 in France, at the UN Climate
26 Change Conference, where parties committed to take ambitious actions to keep global temperature rise
27 below 2°C by the end of the Century (UN, 2016).

28 Hence, the monitoring and the analysis of the temperature rise, at the global, regional or local levels,
29 have been a challenge for the scientific community. Global and European average time series for monthly
30 temperature have been gridded using different interpolation techniques; and the results unveiled that there
31 has been especially relevant climate change in the Iberian Peninsula. Indeed, a high warming has been
32 observed in the past 50 years over the Iberian Peninsula and, over the past 30 years it occurred mainly in
33 summer, EEA (2018). Hence, in the European context the analysis of local time series has a special interest
34 in order to monitor temperature rise. Furthermore, the analysis of these time series avoids interpolation
35 uncertainties associated with global or regional time series.

36 Temperature data can be daily, monthly or annual depending on both the scale, nature, and the theme
37 under consideration. Several studies based on different types of periodicity of data have also been considered
38 in the literature. For instance, the following works were based on daily temperature data: Poppick et al.
39 (2016) studied changes in the distribution of daily temperatures in an ensemble of general circulation model
40 (GCM) runs predicting changes in both means and variability; Trevin (2013) developed a new homogenized

41 daily maximum and minimum temperature data set for Australia; among others (Fischer, 2015; Kleiber
42 et al., 2013; Ngo and Horton, 2016; Trigo and Palutikof, 1999; Wang et al., 2013).

43 A considerable volume of research based on monthly temperature data has also been published. Con-
44 sidering monthly means of daily minimum temperature and daily maximum temperature data from Albert
45 Park, Auckland from 1910 to 1986, Withers and Nadarajah (2015) analyzed the efficiency of modeling
46 observations that are grouped into weekly means, monthly means and annual means. Monthly average
47 temperature series in two widely separated European cities, Lisbon (1856–1999) and Prague (1841–2000),
48 were examined in Alpuim and El-Shaarawi (2009). Other works investigated monthly temperatures (Abbas-
49 nia and Toros, 2016; Bengtsson and Cavanaugh, 2008; Liu et al., 2016; Reich, 2012; William et al., 2012).
50 Annual temperatures were investigated in Xu et al. (2015), and Moreno et al. (2013) analyzed the change
51 points in the annual mean temperature in central England between 1659 and 2011 using a consistent online
52 Bayesian procedure for detecting change points.

53 The most applied statistical models in the analysis of climate time series, in particular of temperatures
54 data sets, are the linear models and time series models such as Autoregressive Integrated Moving Average
55 models (ARIMA) (Alpuim and El-Shaarawi, 2009; Bližňák et al., 2015; Freitas et al., 2015). As an extension
56 of the linear models, state space models have been largely applied to the modeling of environmental data,
57 since they incorporate a versatile stochastic structure that allow for the integration of temporal dependence.
58 The statistical robustness and predictive ability of state space models make them the most promising
59 avenue towards a new type of modern statistical modeling (Patterson et al., 2008). State space models
60 are commonly used to analyze data sets with measurement errors as environmental data (temperature,
61 precipitation, etc.) (Tandeo et al., 2011). Recent works have considered a state space approach to model
62 temperature time series data sets. An additive, structural state-space model was considered in Bengtsson
63 and Cavanaugh (2008) in order to represent the monthly temperature mean as a sum of an overall constant
64 mean, a seasonal component, a monthly temperature anomaly, and a white noise term. An extension of the
65 linear and Gaussian state space was proposed in Tandeo et al. (2011) to analyze time series with irregular

66 time sampling in the modeling of sea surface temperature data from a particular satellite. The monthly
67 minimum temperatures in the State of Rio de Janeiro were analyzed by [Castro Morales et al. \(2013\)](#) using
68 a spatial-temporal model, whose temporal trend is modeled through state space models.

69 This paper is organized as follows. Section 2 introduces methodological aspects, namely, the model
70 description, the periodic Kalman filter version, the parameters estimation and inference aspects. In Section
71 3 an application to three Portuguese cities (Lisbon, Oporto and Coimbra) is presented. Data analyzed
72 was studied by [Morosova and Valente \(2012a\)](#) in order to detect and correct non-climatic homogeneity
73 breaks, long-term temperature data series measured in these three Portuguese cities. These three datasets
74 are available for studies of climate variability in [Morosova and Valente \(2012b\)](#). The work finishes with a
75 discussion of the results in Section 4.

76 2 The Periodic Mixed Linear State Space Model

77 In this section a state space model is proposed, which incorporates a flexible structure in order to accom-
78 modate the different characteristics of the monthly temperature data. Nevertheless, the proposed model
79 is presented in a general form which allows for its adaption to other datasets in different contexts of the
80 environmental area or, for instance, of the economic area.

81 2.1 The model

82 The *Periodic Mixed Linear State Space* (PMLSS) model considers an observable variable Y that is collected
83 with a regular sampling procedure, i.e., the model assumes equidistant time in observations. Usually, the
84 variable Y is observed during N years and each year has S seasons. Thus, we denote $Y_t \equiv Y_{s,n}$ with
85 $t = 1, 2, \dots, T$, $n = 1, 2, \dots, N$ and $s = 1, 2, \dots, S$, where n is the year associated with time t and s is the
86 respective season. With this notation, when t corresponds to the first season of year n than the previous time,
87 which is the season S of year $n - 1$, can be denoted, to simplicity, as season 0 of year n , i.e., $Y_{0,n} \equiv Y_{S,n-1}$.

88 The model is formulated as follows:

$$Y_{s,n} = [1 \quad S(n-1) + s] \begin{bmatrix} a_{s,n} \\ X_{s,n} \end{bmatrix} + D_{s,n}\beta + e_{s,n} \quad (1)$$

$$\begin{bmatrix} a_{s,n} \\ X_{s,n} - \mu_s \end{bmatrix} = \begin{bmatrix} \phi_a & 0 \\ 0 & \phi_s \end{bmatrix} \begin{bmatrix} a_{s-1,n} \\ X_{s-1,n} - \mu_{s-1} \end{bmatrix} + \begin{bmatrix} \omega_{s,n} \\ \varepsilon_{s,n} \end{bmatrix}. \quad (2)$$

89 In the *observation equation*, Eq. 1, the observable variable $Y_{s,n}$ represents the temperature observation
90 in the s^{th} season of the n^{th} year, that is, the $[S(n-1) + s]^{\text{th}}$ observation of the time series. The line matrix
91 $\mathbf{H}_{s,n} = [1 \quad S(n-1) + s]$ is a design matrix of known values, where $S(n-1) + s$ represents the time. The
92 random vector $\mathbf{X}_{s,n} = [a_{s,n} \quad X_{s,n}]'$ has a Periodic Vector Autoregressive of order 1 structure, PVAR(1),
93 and it includes a non-periodic autoregressive process, $a_{s,n} = a_t$, to incorporate the serial correlation; and the
94 Periodic Autoregressive Process of order 1, PAR(1), $X_{s,n}$ that represents the stochastic slopes. The seasonal
95 pattern is incorporated by fixed seasonal coefficients through vector $\beta = [\beta_1 \beta_2 \dots \beta_S]'$, (e.g., $S = 12$ in the
96 case of monthly data). However, these seasonal fixed effects associated to the stochastic slopes in the trend
97 component causes the seasonal pattern to change over time. The $1 \times S$ line matrix $D_{s,n}$ is a design matrix
98 with zeros and ones, as an indicator function in order to associate the respective seasonal coefficient β_s ,
99 with $s = 1, 2, \dots, S$, to the variable $Y_{s,n}$. The observation error $e_{s,n}$ is a Gaussian white noise process with
100 variance $\text{Var}(e_{s,n}) = \sigma_e^2$.

In the *state equation*, Eq. 2, the *state* vector $\mathbf{X}_{s,n}$ follows a PVAR(1) process with mean $\mu_{\mathbf{X}_{s,n}} = [0 \quad \mu_s]'$, where μ_s is the mean of the slope of season s ; Φ_s is the autoregressive matrix $\Phi_s = \text{diag}\{\phi_a, \phi_s\}$, where ϕ_a is the autoregressive coefficient of the AR(1) process, $\{a_{s,n}\}$, and ϕ_s is the autoregressive coefficient associated with the slope of the season s . The vector of errors $\zeta_{s,n} = [\omega_{s,n} \quad \varepsilon_{s,n}]'$ has a multivariate

Gaussian distribution with a covariance matrix $\Sigma_{\zeta_{s,n}} = \text{diag}\{\sigma_{\omega}^2, \sigma_{\varepsilon,s}^2\}$, such that,

$$\text{Cov}(\varepsilon_{s,n}, \varepsilon_{s-i,n}) = \begin{cases} \sigma_{\varepsilon,s}^2, & i = 0 \\ 0, & i \neq 0 \text{ for } i = 1, 2, \dots, S \end{cases}$$

101 and processes $\{\omega_{s,n}\}$ and $\{\varepsilon_{s,m}\}$ are uncorrelated, that is $E(\omega_{s,n}\varepsilon_{r,m}) = 0$, for all s, r, n and m . When in
 102 the AR(1) process $\{a_{s,n}\}$ $|\phi_a| < 1$, which represents the serial correlation, the process is stationary with
 103 zero mean and variance $\text{Var}(a_{s,n}) = \sigma_{\omega}^2(1 - \phi_a^2)^{-1}$.

104 The PAR(1) process, $\{X_{s,n}\}$, which represents the periodic stochastic slopes, is cyclostationary when
 105 $\left| \prod_{k=1}^S \phi_k \right| < 1$, ([Gardner et al., 2006](#); [Monteiro et al., 2010](#); [Obeysekera and Salas, 1986](#)). In this case,
 106 $E(X_{s,n}) = \mu_s$ and

$$\text{Var}(X_{s,n}) = \sigma_s^2 = \left\{ \sigma_{\varepsilon,s}^2 + \sum_{i=1}^{S-1} \left(\prod_{j=1}^i \phi_{s-j}^2 \sigma_{\varepsilon,s-i}^2 \right) \right\} \left(1 - \prod_{k=1}^S \phi_k^2 \right)^{-1}, \quad (3)$$

107 with the convention $\phi_{-i} = \phi_{S-i}$ and $\sigma_{\varepsilon,-i}^2 = \sigma_{\varepsilon,S-i}^2$, for $i = 0, 1, \dots, S-1$.

108 The model (1) – (2) assumes the periodic mixed effect state space representation

$$Y_{s,n} = \mathbf{H}_{s,n} \mathbf{X}_{s,n} + D_{s,n} \beta + e_{s,n} \quad (4)$$

$$\mathbf{X}_{s,n} = \mu_{\mathbf{X}_{s,n}} + \Phi_s(\mathbf{X}_{s-1,n} - \mu_{\mathbf{X}_{s-1,n}}) + \zeta_{s,n}. \quad (5)$$

109 The model (4)–(5) allows for the incorporation of some characteristics which make the model versatile.
 110 Furthermore, this state space formulation associated to the Kalman filter deals well with missing values,
 111 since the maximum likelihood estimates can be obtained through the EM-algorithm. In the temperature
 112 modeling context, the mixed effects approach associated with the intra-annual seasonality is a simple way
 113 of modeling the seasonality that naturally exists in this variable. For instance, in [Kokic et al. \(2011\)](#) the

114 potential of using a linear mixed-effect state-space model for statistical downscaling of climate variables
 115 compared to the frequently used approach of linear regression is shown; [Ursu and Pereau \(2016\)](#) considered
 116 Seasonal Autoregressive Moving Average (SARMA) models which represent a class of stationary models with
 117 large lag autocorrelations that are invariant with respect to the season. However, it is reasonable to admit
 118 that the long-term temperature time series have rises with periodic mean and covariance functions with
 119 respect to time. Therefore, the use of periodic autoregressive modeling of the slope of the temperature time
 120 series linear trend is an appropriate option. Nevertheless, when there are good estimates of periodicities,
 121 one may first deseasonalize the data and then model the resulting temperatures anomalies.

122 2.2 The Kalman filter adaptation to the PMLSS model

123 A state space model has, in its structure, a latent process, the state, which is not observable and needs to
 124 be predicted. The most usual procedure for this prediction is the Kalman filter algorithm. This algorithm
 125 computes, at each time, the optimal estimator of the state vector based on the available information until
 126 t and its success lies on the fact that it is an online estimation procedure. The optimal properties can be
 127 guaranteed only when all model's parameters Θ are known and the normality of errors is valid ([Harvey, 1996](#);
 128 [Shumway, 2017](#)). However, if the normality is dropped, then the Kalman filter predictors are the best linear
 129 unbiased estimators (BLUE). When parameters of the state space model are estimated, the uncertainty
 130 associated with the Kalman filter estimators are underestimated and some procedures can be implemented
 131 ([Costa and Monteiro, 2016](#); [Rodríguez and Ruiz, 2012](#)).

132 Briefly, the Kalman filter is an iterative algorithm that produces, at each time, an estimator of the state
 133 vector $\mathbf{X}_{s,n}$, which is given by the orthogonal projection of the state vector onto the observed variables up
 134 to that time. Considering the matrix representation of the PMLSS model (4) – (5), let $\widehat{\mathbf{X}}_{s|s-1,n}$ denote the
 135 estimator of $\mathbf{X}_{s,n}$ based on the observations $Y_{1,1}, Y_{2,1}, \dots, Y_{s-1,n}$ and let $\mathbf{P}_{s|s-1,n}$ be its covariance matrix,
 136 i.e. $E[(\widehat{\mathbf{X}}_{s|s-1,n} - \mathbf{X}_{s,n})(\widehat{\mathbf{X}}_{s|s-1,n} - \mathbf{X}_{s,n})']$, the Mean Square Error (MSE) matrix. Since the orthogonal

137 projection is a linear estimator, the forecast of the observable vector $Y_{s,n}$ is given by

$$\widehat{Y}_{s|s-1,n} = \mathbf{H}_{s,n} \widehat{\mathbf{X}}_{s|s-1,n} + D_{s,n} \beta \quad (6)$$

138 with MSE given by $\omega_{s,n} = \mathbf{H}_{s,n} \mathbf{P}_{s|s-1,n} \mathbf{H}'_{s,n} + \sigma_e^2$.

139 When $Y_{s,n}$ is available, the prediction error or *innovation*, $\eta_{s,n} = Y_{s,n} - \widehat{Y}_{s|s-1,n}$, is used to update the
140 estimate of $\mathbf{X}_{s,n}$ (*filtering*) through the equation

$$\widehat{\mathbf{X}}_{s|s,n} = \widehat{\mathbf{X}}_{s|s-1,n} + \mathbf{K}_{s,n} \eta_{s,n}, \quad (7)$$

141 where $\mathbf{K}_{s,n}$ is called the Kalman gain matrix and is given by $\mathbf{K}_{s,n} = \mathbf{P}_{s|s-1,n} \mathbf{H}'_{s,n} \omega_{s,n}^{-1}$. Furthermore, the
142 MSE of the updated estimator $\widehat{\mathbf{X}}_{s|s,n}$, represented by $\mathbf{P}_{s|s,n}$, verifies the relationship $\mathbf{P}_{s|s,n} = \mathbf{P}_{s|s-1,n} -$
143 $\mathbf{K}_{s,n} \mathbf{H}_{s,n} \mathbf{P}_{s|s-1,n}$. The forecast for the state vector $\mathbf{X}_{s+1|s,n}$ is given by the equation

$$\widehat{\mathbf{X}}_{s+1|s,n} = \mu_{s+1} + \Phi_{s+1} (\widehat{\mathbf{X}}_{s|s,n} - \mu_s) \quad (8)$$

144 and its MSE matrix is $\mathbf{P}_{s+1|s,n} = \Phi_{s+1} \mathbf{P}_{s|s,n} \Phi'_{s+1} + \Sigma_{\zeta_{s,n}}$.

145 The Kalman filter algorithm is initialized with $\mathbf{X}_{1|0,1}$ and $\mathbf{P}_{1|0,1}$. When the state process is stationary,
146 the Kalman filter algorithm can be initialized considering that initial state vector $\widehat{\mathbf{X}}_{1|0,1} = \text{diag}\{0, \mu_1\}$ and
147 the covariance matrix $\mathbf{P}_{1|0} = \text{diag}\{\sigma_\omega^2, \sigma_1^2\}$ according to Eq. 3. In the non-stationarity case, the initialization
148 of the Kalman filter can be incorporated in the estimation procedure or can be specified in terms of a diffuse
149 or non-informative prior (Harvey, 1996).

150 2.3 Gaussian maximum likelihood estimation of parameters

151 Under the assumptions that the initial state, the state noise process $\{\varepsilon_{s,n}\}$ and the observation noise process
152 $\{e_{s,n}\}$, are normal and mutually independent and considering, without loss of generality, N complete years

153 in the realization $\mathcal{Y} = (Y_{1,1}, Y_{2,1}, \dots, Y_{S,N})'$, the logarithm of the conditional Gaussian likelihood function is
 154 computed as follows

$$\log(\mathcal{L}(\Theta; \mathcal{Y})) = -\frac{NS}{2} \log(2\pi) - \frac{1}{2} \sum_{n=1}^N \sum_{s=1}^S \log(\omega_{s,n}) - \frac{1}{2} \sum_{n=1}^N \sum_{s=1}^S \frac{\eta_{s,n}^2}{\omega_{s,n}}, \quad (9)$$

155 where $\Theta = (\beta_1, \dots, \beta_S, \sigma_e^2, \mu_1, \dots, \mu_S, \phi_a, \phi_1, \dots, \phi_S, \sigma_\omega^2, \sigma_{1,\varepsilon}^2, \dots, \sigma_{S,\varepsilon}^2)'$ is the τ -vector, $\tau = 4S+3$, of the unknown
 156 parameters to be estimated.

157 The maximum likelihood (ML) estimates are obtained upon maximizing the log-likelihood function, that
 158 is, $\Theta_{\text{ML}} = \text{argmax}_{\Theta} \log(\mathcal{L}(\Theta; \mathcal{Y}))$. As the log-likelihood function $\log(\mathcal{L})$ is nonlinear, it is possible to obtain
 159 the ML estimates using numerical algorithms. Further details on parameters estimation can be obtained in
 160 the Appendix.

161 **3 Application to homogenized monthly time series of air temperature**

162 In this section, we apply the periodic mixed linear state space modeling to the homogenized monthly time
 163 series of air temperature in three Portuguese cities produced by [Morosova and Valente \(2012a\)](#) and available
 164 in [Morosova and Valente \(2012b\)](#). Based on these time series, we constructed monthly mean temperature
 165 series based on maximum and minimum of the homogenized time series.

166 **3.1 Data description**

167 This section provides a description of the data that motivates this study. [Morosova and Valente \(2012a\)](#)
 168 developed and provided a data set with long-term time series of monthly data of temperatures in the three
 169 Portuguese cities. This data set is the result of a procedure that detected and corrected non-climatic ho-
 170 mogeneity breaks in an original data set. As mentioned by these authors [Morosova and Valente \(2012a\)](#),
 171 long instrumental climatological records assume a paramount role in the studies of atmospheric conditions

172 variation, providing vital information about climate variability, trends and cycles. However, long-term series
173 often contain inhomogeneities originated by changes in instruments, station locations and surrounding envi-
174 ronment, observation routines and methods of preliminary data treatment. Thereof, the data set available
175 after the detection and correction of these inhomogeneities is useful to develop accurate climate studies.
176 The procedure adopted in [Morosova and Valente \(2012a\)](#) is based, in a first step, on statistical methods for
177 detection of non-climatic breaks and their corrections dT were computed considering time interval around
178 the break and smoothing of 12 monthly correction values dT by 3-month adjacent averaging to achieve a
179 reasonable variation of dT throughout the year; so, the correction of each time series only depends on itself.

180 The work developed in [Morosova and Valente \(2012a\)](#) produced a set of homogenized time series of
181 monthly averages of daily minimum (T_{min}) and daily maximum (T_{max}) temperatures in three Portuguese
182 cities – Lisbon, Oporto and Coimbra– based on the original data sets, which were tested in order to detect
183 and correct the homogeneity breaks. Our work focuses on the monthly mean of the daily mid-range
184 temperature time series, computed as $T_{aver} = (T_{min} + T_{max})/2$. This climatology variable was used in other
185 previous works on temperature evolution in these Portuguese cities, for instance in [Alpuim and El-Shaarawi](#)
186 [\(2009\)](#); [Espírito Santo et al. \(2014\)](#); [Ramos et al. \(2011\)](#); or in other contexts ([Bengtsson and Cavanaugh,](#)
187 [2008](#); [Perry and Hollis, 2005](#)).

188 Relatively to the Oporto data series, the original data set was measured by the *Instituto Geofísico*
189 *(Observatório Meteorológico da Serra do Pilar) da Universidade do Oporto (IGUP)*, from 1888 to 2001,
190 comprising 114 years. The original data series of Lisbon were measured at the *Instituto Geofísico do Infante*
191 *D. Luís (IGIDL)*, from 1856 to 2008, corresponding to a data set length of 153 years. The original data
192 set of Coimbra was measured at the *Instituto Geofísico da Universidade de Coimbra (IGUC)*, from 1865 to
193 2005, with a length of 141 years.

194 Notice that Lisbon, Oporto and Coimbra have different climate characteristics (see geodesic coordinates
195 in [Table 1](#)). While Lisbon has a humid temperate climate with dry and hot summer, Oporto and Coimbra
196 have a temperate climate with dry and mild summers. Nonetheless, Oporto is located along the Atlantic

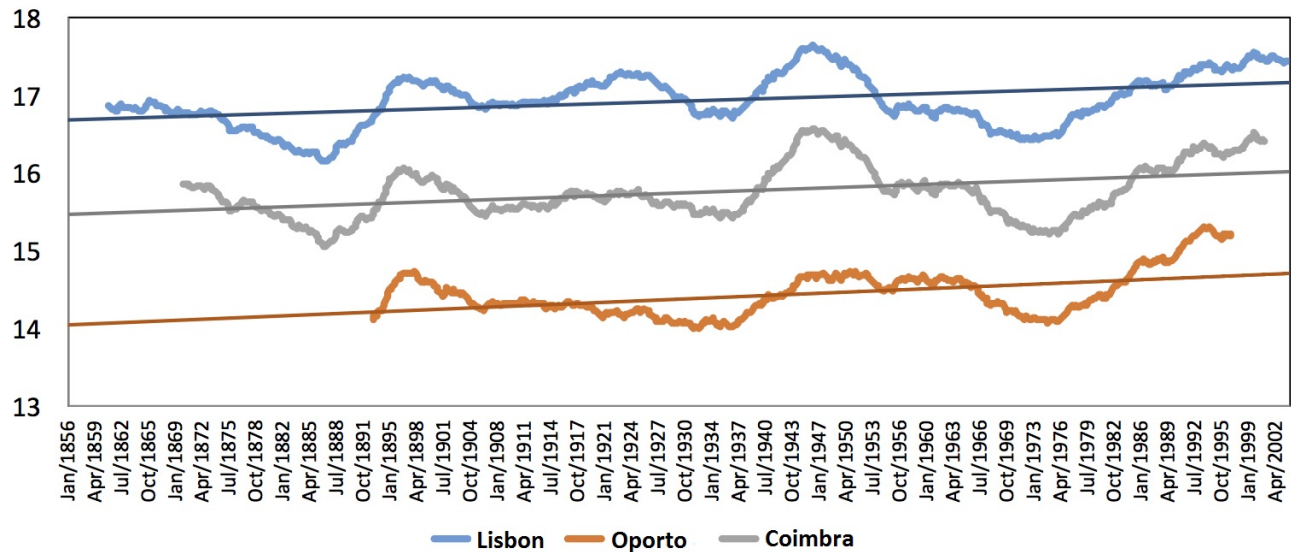


Figure 1: Ten-year moving average temperature series, with a linear trend adjustment.

197 Ocean in the northern coast, while Coimbra is located approximately 40 km from the Atlantic Ocean and
 198 close to the cordillera Montejunto – Serra da Estrela System, highest mountain of mainland Portugal with
 199 an altitude of 1993 m.

200 — table 1 —

201 Since the time series are quite long, Figure 1 shows the 10-year moving average of the time series in order
 202 to facilitate a visual inspection of an over-all behavior. Figure 1 shows that the rise in temperature varies
 203 on time. Figure 2 represents, for each city, the least squares parameters estimates of the 12 linear regression
 204 models to the respective annual time series associated with each month of the year. These estimates indicate
 205 that the temperature rise is not the same through every month of the year. In fact, in the previous work
 206 [Alpuim and El-Shaarawi \(2009\)](#), based on monthly temperatures data of Lisbon (1856–1999), and Prague,
 207 results showed that the rise in temperature is not equal in each month of the year. Thus, this means that
 208 the rise in temperature has two types of variability: from month to month over the year and over time.

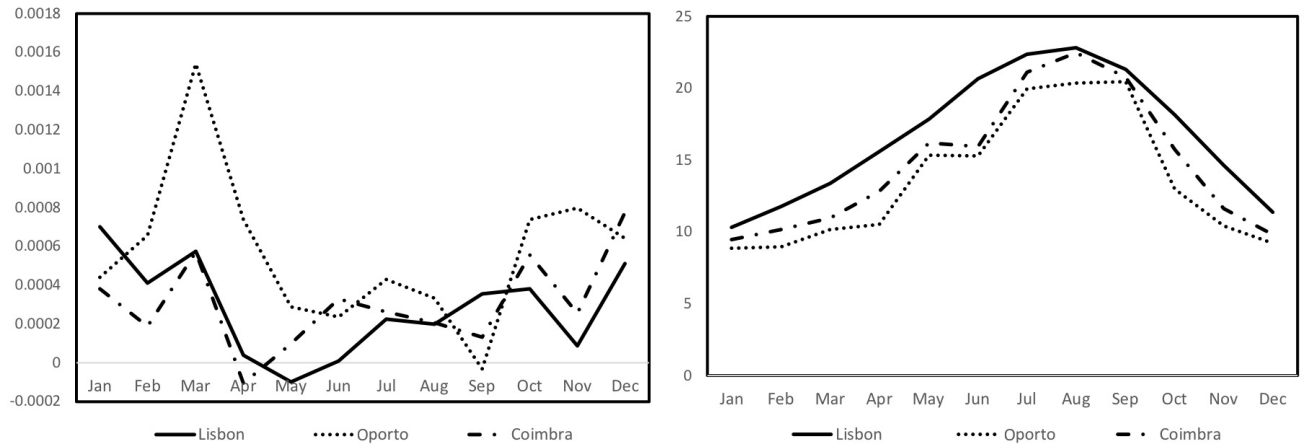


Figure 2: Least squares estimates of the linear model for each month of the year, for each city; (left) estimates of the slopes and (right) estimates of levels.

209 3.2 Models adjustments and validation

210 A first approach to model the time series under analysis was to consider, based on the exploratory analysis
 211 exposed in section 3.1, a PMLSS model (1) – (2) without the autoregressive state $\{a_{s,n}\}$ component, since it
 212 was expected that the serial correlation would be accommodated through the state vector of stochastic slopes
 213 with a PAR(1) structure with $S = 12$ seasons – the months of the year. The log-likelihood maximization
 214 procedure was initialized using the least squares estimates of the linear regression models $Y_t^{(s)} = b_s + t \cdot m_s +$
 215 $\xi_t^{(s)}$, where $t = s + 12k$ for $s = 1, 2, \dots, 12$ and k is an integer, for the monthly subseries. Hence, the initial
 216 values for the fixed effects were the estimated levels, $\hat{\beta}_s^{(0)} = \hat{b}_s$, and for the mean of the periodic stochastic
 217 slopes were the estimated slopes in the regression models, $\hat{\mu}_s^{(0)} = \hat{m}_s$ (see Figure 2).

218 In the initial model validation phase, the analysis of the observed innovations series $\{\hat{\eta}_{s,n}\}$ showed the
 219 existence of a remaining temporal correlation. In fact, both sample autocorrelation (ACF) and partial
 220 autocorrelation (PACF) functions of innovations $\{\hat{\eta}_{s,n}\}$ of this model in three cities (Lisbon, Oporto and
 221 Coimbra) have indicated that there is a temporal correlation. Therefore, innovations series do not present
 222 the characteristics of a white noise as it was assumed; sample ACF and PACF of the innovations series show

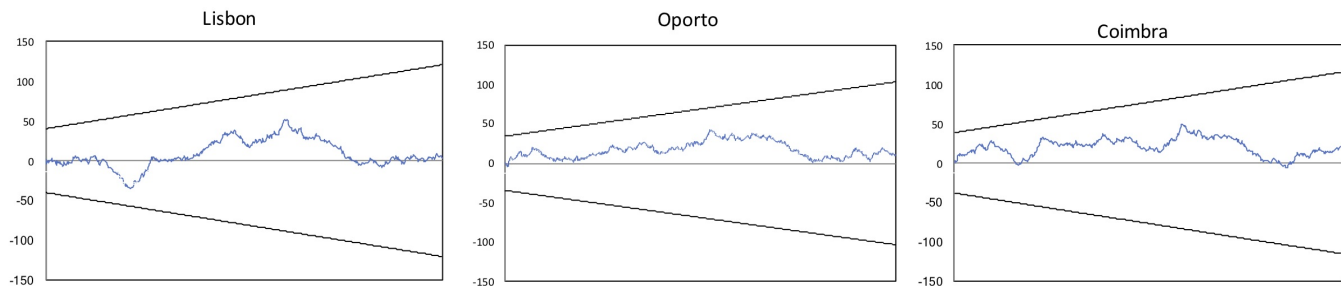


Figure 3: Plots of the cumulative sum (CUSUM).

223 that an autoregressive process should be incorporated into the model under analysis.

224 Thus, the estimation procedure described in Section 2.3 was implemented for three models (1) – (2) with
 225 the autoregressive process, using the Generalized Reduced Gradient (GRG2) method in the maximization
 226 step. In the optimization procedure, several disturbances were added to the initial values in order to assess
 227 the stability of the procedure. In each time series, the maximum likelihood procedure converged, with
 228 several significant digits, to the same solution. Before the discussion and interpretation of the results, a
 229 set of procedures were performed in order to validate the models and to evaluate their assumptions. In
 230 a global analysis, all models adjusted very well to data, since all assumptions are verified and they also
 231 present high values of the respective coefficients of determination. Innovations $\eta_{s,n}$ were assumed to have
 232 a conditional Gaussian distribution $\eta_{s,n} = Y_{s,n} - \widehat{Y}_{s|s-1,n} \sim N(0, \omega_{s,n})$. The normality of residuals series
 233 were tested considering both the Kolmogorov–Smirnov (K-S) test and the Jarque–Bera (JB) test. In all
 234 cases, normality was not rejected considering the usual 5% to the significance. In fact, in the K-S test ,all
 235 p-values were greater than 0.20 and in the JB test p-values were equal to 0.74, 0.21 and 0.10, respectively
 236 for Lisbon, Oporto and Coimbra. Moreover, histograms and QQ-plots with 95% confidence envelopes of
 237 standardized innovations allow to conclude that their empirical distributions are consistent with the Gaussian
 238 curve. Furthermore, the three innovations series did not present serial correlation, as assumed, since empirical
 239 ACF and PACF indicated that innovations are compatible with a white noise process.

240 Moreover, plots of cumulative sum (CUSUM) with a significance level of 5% were obtained to three
 241 residuals series. A considerable amount of information can be obtained simply by inspecting these plots; the
 242 CUSUM procedure is particularly valuable for detecting structural change (Harvey, 1996). Figure 3 shows
 243 the plots of CUSUM and the graphical analysis indicates that there are no structural changes in residuals
 244 series.

245 In order to assess models adjustment, coefficients of determination associated with the one-step ahead
 246 forecasts were computed, i.e., $r^2 = \text{corr}(Y_{s,n}; \widehat{Y}_{s|s-1,n})^2$. All models have coefficients of determination greater
 247 than 90%. Indeed, in Lisbon, the adjusted model has a coefficient of determination for the one-step-ahead
 248 forecast of $r^2 = 0.937$, while, in Oporto, this coefficient is $r^2 = 0.919$ and in Coimbra $r^2 = 0.922$ (see Table
 249 2).

250 — TABLE 2 —

251 Furthermore, for each model the coverage probability for the empirical one-step-ahead 95% confidence
 252 intervals were computed and are close to the confidence level considered. The coverage probability values
 253 were 95.15%, 95.76% and 94.98%, in Lisbon, Oporto and Coimbra, respectively.

254 3.3 Warming rates estimates based on the PMLSS models adjustment

255 Figure 4 represents the estimated curves of the seasonal fixed effects according to the Gaussian maximum
 256 likelihood estimates of β_i , with $i = 1, 2, \dots, 12$. These estimates show that Lisbon and Coimbra have a similar
 257 pattern over the year, nonetheless Lisbon has the highest values of monthly means. Results associated with
 258 Oporto indicate that the annual temperature curve in this city has a different pattern in comparison with
 259 the other two cities and also that Oporto has comparatively the lowest monthly values of temperature.

260 The monthly means μ_s , with $s = 1, 2, \dots, 12$, of the stochastic slopes $X_{s,n}$, have an environmental special
 261 interest, since they quantify the monthly rise of the long-term temperature time series. Note that these
 262 parameters are the mean parameters of the PAR(1) model. For each month s , based on the ML estimate
 263 of $\widehat{\mu}_s$, we compute $100 \times 12 \times \widehat{\mu}_s$, which are represented in Figure 5 (see also Table 3), in order to compare

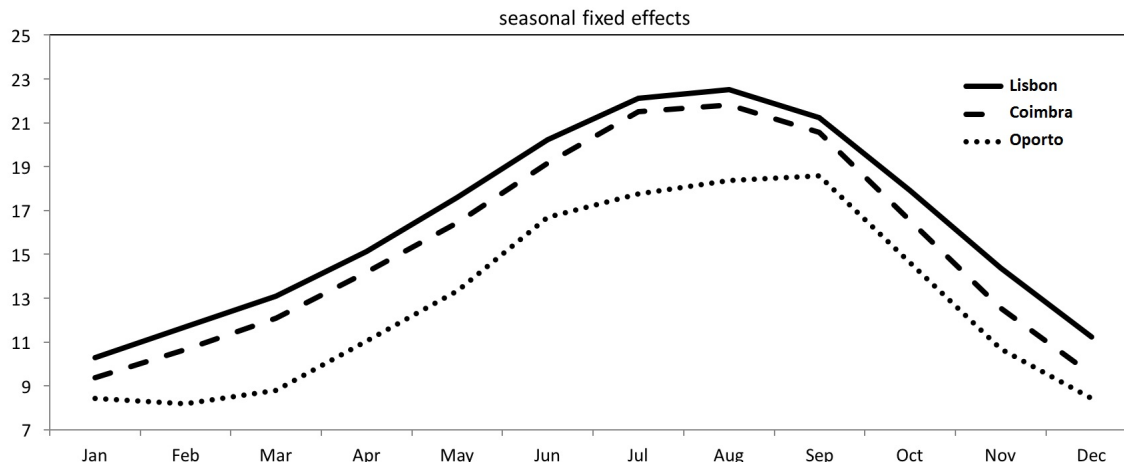


Figure 4: Maximum likelihood estimates of the seasonal fixed effects of temperature for Lisbon, Oporto and Coimbra.

264 the mean rise of temperature in the different cities using a reference time unit. These values represent
 265 12 estimates of the mean rise of temperature in 100 years, that is, a mean rise per century. Hence, their
 266 average is an estimate of the mean increase of annual temperature in a century, $1/12 \sum_{s=1}^S (100 \times 12 \times \hat{\mu}_s) =$
 267 $100 \times 12 \times \hat{\mu}$. In fact, if we compute, for each time series (city), the overall monthly mean rise of temperature
 268 $\mu = 1/12 \sum_{s=1}^{12} \mu_s$, then the mean μ_s in the PMLSS model can be rewritten as $\mu_s = \mu + \mu_s^*$, where μ is the
 269 overall monthly mean rise of temperature and μ_s^* is the effect of the month s , with $\sum_{s=1}^{12} \mu_s^* = 0$.

270 —TABLE 3—

271 The adjusted model for Lisbon estimates the mean increase, per century, in the annual temperature
 272 at 0.621°C , whereas in the corresponding models for Coimbra and Oporto the estimate is 0.545°C and
 273 2.166°C , respectively. The annual rise in temperature in Lisbon and Coimbra is similar and less than 1°C ,
 274 while in Oporto we estimated a rise exceeding 1°C , per century. Relatively to Lisbon, we can compare
 275 the annual rise of temperature with two other works. In the first work, [Alpuim and El-Shaarawi \(2009\)](#)
 276 used linear models with correlated errors to model Lisbon monthly temperatures time series between 1856

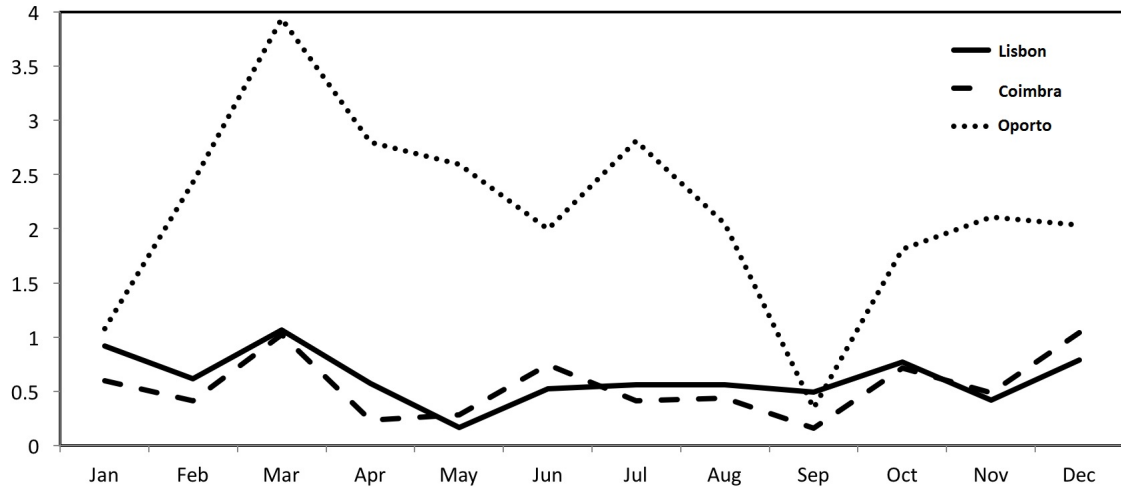


Figure 5: Estimates of monthly warming rates, per cent, in Lisbon, Oporto and Coimbra.

277 and 1999 collected at the Climatological Archive of the Portuguese Meteorological Institute and they have
 278 obtained the value of 1.024°C as an estimate to the annual rise per cent. That is, the adjusted PMLSS
 279 model to the homogenized data produced by [Morosova and Valente \(2012a\)](#) obtained a lower estimate than
 280 [Alpuim and El-Shaarawi \(2009\)](#), although both indicate a mean rise of temperature in Lisbon in the last
 281 decades. The linear model that was applied only considered a AR(1) structure in residuals series, once
 282 slopes are deterministic, whereas in the PLMSS model two types of serial correlation were considered: a
 283 VAR(1) structure in slopes and a month-to-month AR(1) structure. More recently, [Costa and Monteiro](#)
 284 [\(2015\)](#) obtained an estimate of the mean rise of 0.427°C , per cent, in Lisbon, based on the same dataset
 285 of this work considering a dynamic linear model without a periodic structure for the stochastic slopes, which
 286 may explain the difference between both estimates.

287 Regarding the Oporto and Coimbra monthly mean temperature data, there are no other studies which
 288 allow us to make a direct comparison. In fact, the Lisbon series is usually chosen to make comparative
 289 European or global climate studies, because it is the best documented series and is generally considered
 290 representative of the Portuguese average climate, although one should keep in mind that there may be some

291 regional variations (Miranda et al., 2002). In a more thorough analysis, we can also observe the estimates
 292 of monthly mean rises in temperature for each month of the year since this value changes according to the
 293 month. In Lisbon, from April until September, the temperature rise is less than the annual rise average,
 294 whereas between December and March the temperature rise have values on average or greater than the
 295 annual average. So, mean temperatures are increasing every month, but the warming rate in winter months
 296 is greater. The largest warming rate per century is found in March with an estimated value of 1.066°C
 297 and the lowest warming rate is estimated in May with the value of 0.167°C . The monthly mean rises of
 298 temperature in Coimbra are close to the corresponding values in Lisbon time series and with a similar shape
 299 (empirical linear correlation of $r = 0.700$). In Coimbra, the largest warming rate per century is in December
 300 with 1.044°C , very close to the estimate rise in March with 1.024°C . Nevertheless, the lowest warming rate
 301 per century is found in September with 0.158°C . In Oporto, eventhough annual warming is more significant
 302 than in Lisbon or Coimbra, results show that there is a clear annual cycle in the warming rate. In fact,
 303 excluding June, which has a rate similar to the annual average, the remaining months (between February and
 304 July) have warming rates greater than the annual rate average, while from August until January warming
 305 rates are lower. Therefore, in Oporto there are two periods of the year with different warming rates.

306 3.4 Global analysis of the adjusted models

307 The proposed PMLSS model has three types of variability sources. One is related to the errors of the
 308 periodic state associated with the stochastic slopes, $\varepsilon_{s,n}$, with variance $\sigma_{\varepsilon,s}^2$; another is associated with the
 309 error $\omega_{s,n}$ of the autoregressive process $\{a_{s,n}\}$; and the last source of variability is the observation error $e_{s,n}$
 310 with variance σ_e^2 .

311 — TABLE 4 —

312 Table 4 presents Gaussian maximum likelihood estimates of all variances present in the PMLSS models.
 313 Lisbon and Coimbra have observations errors $e_{s,n}$ with similar estimates of their variances while in the
 314 time series of temperatures of Oporto this estimate is greater. Coimbra presents, each month, the highest

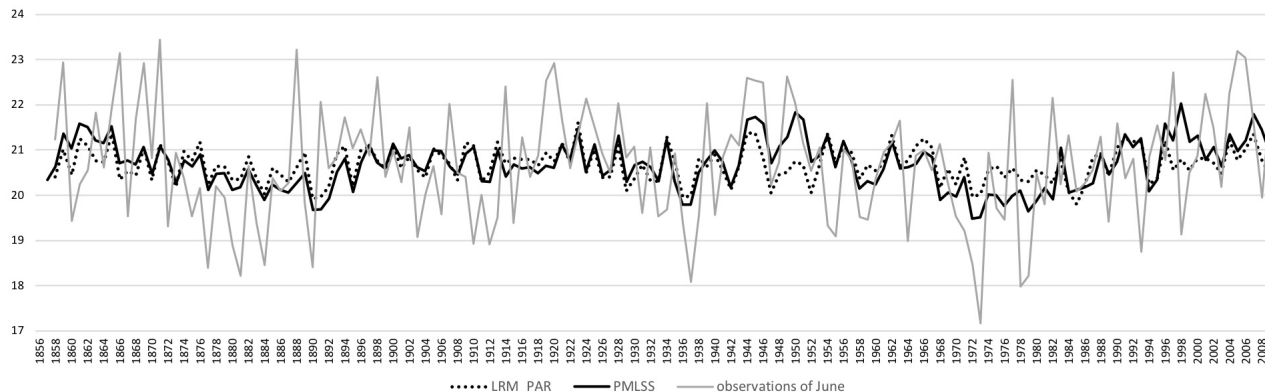


Figure 6: Trend estimates of June in Lisbon obtained by PMLSS model and the multiple linear regression model with PAR errors.

315 estimated variance of the periodic state errors. As expected, the autoregressive processes $a_{s,n}$ has errors
 316 with small variances, since this component incorporates the month-to-month serial correlation. Estimates
 317 of the autoregressive parameters involved in the PMLSS model are presented in Table 5. On the one hand,
 318 all three autoregressive processes $a_{s,n}$ are estimated as stationary, since estimates of ϕ in three cities verify
 319 comfortably the stationarity condition $|\hat{\phi}| < 1$. On the other hand, the PAR(1) process, that represents the
 320 periodic stochastic slopes, is stationary as well, since we have $\prod_{s=1}^{12} \hat{\phi}_s < 1$ in Lisbon, Coimbra and Oporto.

321 — TABLE 5 —

322 A competing multiple linear regression model with PAR(1) errors, MLR_PAR, was adjusted to perform
 323 a comparison of trends estimates. This model is an improvement of the linear regression model considered
 324 in the initialization of the log-likelihood maximization procedure, that is, $Y_{s,n} = b_s + t \cdot m_s + \xi_{(s,n)}$ where
 325 $\xi_{(s,n)}$ follows a PAR(1) process. Analyzing the PMLSS model trend estimates justaposed against MLR_PAR
 326 trends estimates, we concluded that the these estimates are more similar when the month's subseries trend
 327 is approximately linear (fixed). Unlike this, when in a month trend is not linear, the PMLSS model captures
 328 these changes in a more dynamic way than the MLR_PAR model. For instance, Figure 6 shows trend
 329 estimates of June in Lisbon obtained by PMLSS model and the MLR_PAR. The PMLSS model has a PAR

330 structure in the slopes process, which allows for local linear trends, while the MLR_PAR model incorporates
 331 a periodic structure in errors.

332 Since PMLSS models adjusted very well to three time series, their structural components can be used
 333 to monitor the rise in temperature both in a large scale, for instance in a secular period as was done before,
 334 or in a on-line procedure, that is, in a month-to-month analysis.

335 In an online scheme, the Kalman filter provides one-step-ahead forecasts for monthly temperature,
 336 $\hat{Y}_{s|s-1,n}$ with the respective empirical confidence intervals at $(1 - \alpha) \times 100\%$ level

$$Y_{s,n} = \hat{Y}_{s|s-1,n} \pm z_{1-\frac{\alpha}{2}} \sqrt{\hat{\omega}_{s,n}}$$

where $z_{1-\alpha/2}$ represents the normal quantile of probability $1 - \alpha/2$. The unobservable structural components can be predicted through the Kalman filter equation and the associated confidence intervals. Hence, confidence intervals for the stochastic slopes, $\{X_{s,n}\}$, can be computed through

$$X_{s,n} = \hat{X}_{s|s,n} \pm z_{1-\frac{\alpha}{2}} \sqrt{\hat{p}_{s|s,n}^{(2,2)}}$$

while the confidence interval for the AR(1) process, $\{a_{s,n}\}$, which incorporates the month-to-month serial correlation is

$$a_{s,n} = \hat{a}_{s|s,n} \pm z_{1-\frac{\alpha}{2}} \sqrt{\hat{p}_{s|s,n}^{(1,1)}}$$

337 where $\hat{p}_{s,n}^{(i,i)}$ represents the i th element, with $i = 1, 2$, of the diagonal of the MSE matrix $\hat{\mathbf{P}}_{s|s,n}$.

338 Figure 7 represents predictions with the respective empirical 95% confidence intervals of the monthly
 339 mean temperature in Lisbon and the filtered predictions of the unobservable components obtained with the
 340 adjusted PMLSS model in last decade of available data. These results allow for the monitoring of monthly
 341 rise of temperature in mean temperature measurement, as well as in the monthly ratio of warming filtering
 342 errors of observation.

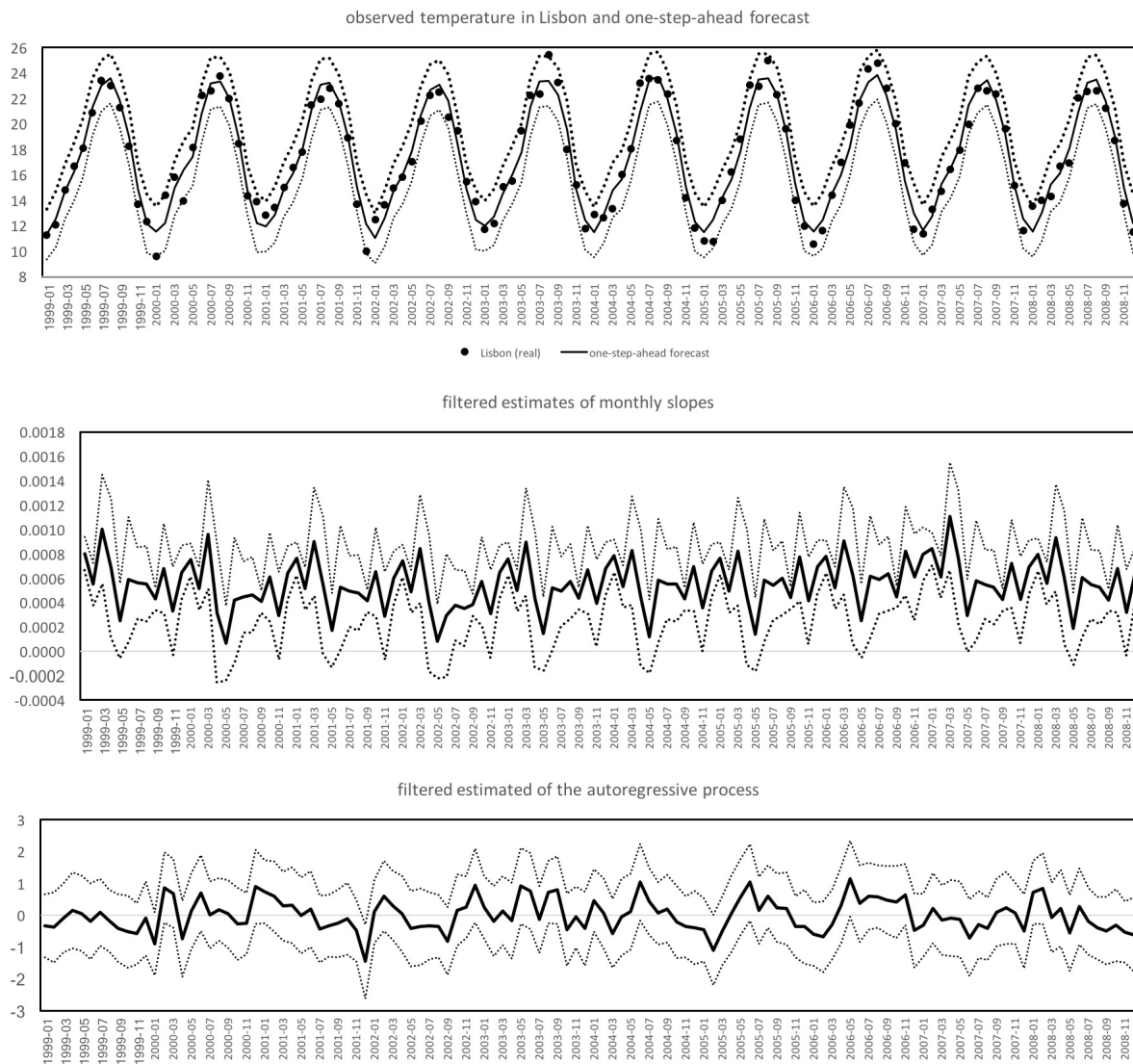


Figure 7: (top) Observed temperature (points) in Lisbon, $Y_{s,n}$, with the one-step-ahead forecast, $\hat{Y}_{s|s-1,n}$; (middle) filtered estimates of the PAR(1) process, $\hat{X}_{s|s,n}$; (below) filtered estimates of autoregressive process, $\hat{a}_{s|s,n}$, with empirical 95% confidence intervals, related to the last decade (January 1999 to December 2008).

343 4 Conclusions and discussion

344 In this work, we have proposed a periodic state space model to analyze long-term temperature time series.
345 The proposed framework incorporates fixed and stochastic effects, namely, the seasonality behavior with fixed
346 levels effects and dynamic slopes over the months of the year. Previous works indicated that temperature rise
347 differs between months, as well as an autoregressive process in order to accommodate the serial correlation.
348 The state space representation allows for the achievement of accurate one-step-ahead forecasts for the
349 monthly mean temperature and for the unobservable structural components, as well as filtered estimates of
350 states. These estimates are computed by a periodic version of the Kalman filter algorithm.

351 The proposed model was adjusted to monthly mean of the daily mid-range temperature long-term time
352 series of three Portuguese cities: Lisbon, Oporto and Coimbra. Main results showed that Lisbon and Coimbra
353 had a similar annual rise of temperature: 0.6212°C and 0.5454°C , per century, respectively. Additionally, it
354 was estimated that, in Oporto, there is a significant mean rise in temperature of 2.1655°C per century. In
355 a more refined analysis, it was found that there is a similarity between mean monthly rises in Lisbon and
356 Coimbra while Oporto has a unique rise pattern. In fact, Oporto has greater warming rates in spring and
357 in the beginning of summer, and lower warming rates at the end of summer until the middle of winter. In
358 Lisbon and Coimbra the biggest warming rates were found in winter and in the beginning of spring and the
359 lowest rise rates were found from the middle of spring until the beginning of autumn.

360 The PMLSS model accommodates the most common properties of environmental. The seasonality is
361 incorporated in two ways: seasonal levels as fixed effects and in the periodic process of monthly slopes; the
362 month-to-month serial correlation is accommodated by an autoregressive process. The proposed model can
363 be improved in order to include spatial-variation when a set of time series of monthly mean temperature
364 are available. If the number of locations is significant and locations are geographically scattered, a spatial
365 structure can be incorporated in the model via the error in the observation equation, through the specification
366 of a spatially structured variance-covariance matrix ([Castro Morales et al., 2013](#)). Alternatively, the spatial

367 structure can be incorporated in an additive way according to an isotropic Gaussian process as proposed in
 368 [Cunha et al. \(2017\)](#).

369 5 Acknowledgements

370 The authors would like to thank the anonymous referees for many helpful critics and suggestions that
 371 contributed to improve this paper. Authors were partially supported by Portuguese funds through the
 372 CIDMA - Center for Research and Development in Mathematics and Applications, and the Portuguese
 373 Foundation for Science and Technology ("FCT- Fundação para a Ciência e a Tecnologia"), within project
 374 UID/MAT/04106/2013.

375 6 Appendix

376 In model (6)–(7) the dimension of the vector of parameters Θ can be quite large, depending on the number
 377 of seasons S of the year that is being considered in the model. Taking into account that temperature data in
 378 this work has a monthly periodic structure, that is $S = 12$, we have $\tau = 51$ parameters to be estimated, which
 379 makes the optimization problem computationally unstable. Hence, in this case a partitioned algorithm with
 380 leapfrog (non-simultaneous) iterations is adopted to replace the original estimation problem into a series of
 381 problems of lower dimension ([Smyth, 1996](#)). Without loss of generality, let's assume that Θ is partitioned
 382 into subvectors Θ_1 and Θ_2 , allowing for the updating equation to be written as

$$\begin{aligned}\Theta_1^{(k+1)} &= \operatorname{argmax}_{\Theta_1} \log(\mathcal{L}_1(\Theta_1^{(k)}, \Theta_2^{(k)}; \mathcal{Y})) \\ \Theta_2^{(k+1)} &= \operatorname{argmax}_{\Theta_2} \log(\mathcal{L}_2(\Theta_1^{(k+1)}, \Theta_2^{(k)}; \mathcal{Y})).\end{aligned}$$

383 In the model under analysis, the natural partition of Θ is considering Θ_1 the fixed effects β_s ; Θ_2 the
 384 slopes averages μ_s , Θ_3 the autoregressive parameters $\phi_s, s = 1, \dots, S$, and ϕ_a and Θ_4 with $S + 2$ variances

385 parameters.

386 So, the ML estimates are computed through the iterative procedure:

387 **Step 1** Obtain least squares estimates of intercept, slope and error variance of a linear trend model for
388 each month, $Y_t^{(s)} = b_s + t \cdot m_s + \xi_t^{(s)}$, and $\xi_t^{(s)}$ is a random error with $\text{var}(\xi_t^{(s)}) = \sigma_{s,\xi}^2$, where $t = s + Sk$
389 for $s = 1, 2, \dots, S$, $k = 0, \dots, N - 1$.

390 **Step 2** Consider initial values to subvector of fixed effects and slopes averages such that $\Theta_1^{(0)} = \{\widehat{b}_1, \dots, \widehat{b}_S\}$
391 and $\Theta_2^{(0)} = \{\widehat{m}_1, \dots, \widehat{m}_S\}$.

392 **Step 3** Initialize the subvector of the autoregressive parameters taking initial values satisfying the cyclo-
393 stationary of the process $\{X_{s,n}\}$ and the AR(1) process, for instance $\phi_k^{(0)} = 0.5^{1/S}$ and $\phi_a^{(0)} = 0.5$, that
394 is, $\Theta_3^{(0)} = \{0.5, 0.5^{1/S}, \dots, 0.5^{1/S}\}$.

395 **Step 4** Take initial values to the subvector of variances $\Theta_4^{(0)} = \{\sigma_e^{2(0)}, \sigma_\omega^{2(0)}, \sigma_{1,\epsilon}^{2(0)}, \dots, \sigma_{S,\epsilon}^{2(0)}\}$ considering the
396 estimates $\widehat{\sigma}_{s,\xi}^2$ as the total variability in each month, for instance, $\widehat{\sigma}_{s,\epsilon}^{2(0)} = \widehat{\sigma}_e^{2(0)} = \widehat{\sigma}_{s,\xi}^2/2$, and a small
397 value to monthly variability of slopes, $(\sigma_\omega^{2(0)} = 10^{-10})$.

398 At this step, vector Θ is fully initialized with values $\Theta^{(0)} = \{\Theta_1^{(0)}, \Theta_2^{(0)}, \Theta_3^{(0)}, \Theta_4^{(0)}\}$;

399 **Step 5** Initialize the periodic Kalman filter according to stationary properties of the state process; without
400 loss of generality, considering that the first observation is related to the season $s = 1$, take $\widehat{\mathbf{X}}_{1|0,1} =$
401 $[0 \quad \widehat{\mu}_1^{(0)}]'$ and $\mathbf{P}_{1|0,1} = \text{diag}\{\widehat{\sigma}_\omega^{2(0)}(1 - \widehat{\phi}_a^{2(0)})^{-1}, \widehat{\sigma}_1^2\}$, where $\widehat{\sigma}_1^{2(0)}$ is computed by Eq. 3.

402 **Step 6** Compute the periodic Kalman filter estimators by equations Eq. (6), Eq. (7) and Eq. (8); and the
403 log-likelihood $\log(\mathcal{L}(\Theta^{(0)}; \mathcal{Y}))$ by Eq. (9).

404 **Step 7** Use a computational routine in order to perform, in a leapfrog algorithm, the direct numerical

405 maximization of the log-likelihood function to obtain $\Theta_j^{(k+1)}$, with $j = 1, 2, 3, 4$, by:

$$\begin{aligned}\Theta_1^{(k+1)} &= \operatorname{argmax}_{\Theta_1} \log(\mathcal{L}_1(\Theta_1^{(k)}, \Theta_2^{(k)}, \Theta_3^{(k)}, \Theta_4^{(k)}; \mathcal{Y})) \\ \Theta_2^{(k+1)} &= \operatorname{argmax}_{\Theta_2} \log(\mathcal{L}_2(\Theta_1^{(k+1)}, \Theta_2^{(k)}, \Theta_3^{(k)}, \Theta_4^{(k)}; \mathcal{Y})) \\ \Theta_3^{(k+1)} &= \operatorname{argmax}_{\Theta_3} \log(\mathcal{L}_3(\Theta_1^{(k+1)}, \Theta_2^{(k+1)}, \Theta_3^{(k)}, \Theta_4^{(k)}; \mathcal{Y})) \\ \Theta_4^{(k+1)} &= \operatorname{argmax}_{\Theta_4} \log(\mathcal{L}_4(\Theta_1^{(k+1)}, \Theta_2^{(k+1)}, \Theta_3^{(k+1)}, \Theta_4^{(k)}; \mathcal{Y}))\end{aligned}$$

406 In this step the parameters estimates are available in iteration $k + 1$, $\Theta^{(k+1)}$.

407 **Step 8** Repeat steps 5 to 7 up to the convergence.

408 References

- 409 Abbasnia, M. and Toros, H. (2016). Future changes in maximum temperature using the statistical down-
410 scaling model (SDSM) at selected stations of Iran. *Model. Earth Syst. Environ.*, 68. doi: 10.1007/s40808-
411 016-0112-z.
- 412 Alpuim, T. and El-Shaarawi, A. (2009). Modeling monthly temperature data in Lisbon and Prague. *Envi-*
413 *ronmetrics*, 20:835–852. doi: 10.1002/env.964.
- 414 Bengtsson, T. and Cavanaugh, J. (2008). State-space discrimination and clustering of atmospheric time
415 series data based on Kullback information measures. *Environmetrics*, 19:103–121. doi: 10.1002/env.859.
- 416 Bližňák, V., Valente, M., and Bethke, J. (2015). Homogenization of time series from portugal and its former
417 colonies for the period from the late 19th to the early 21st century. *International Journal of Climatology*,
418 35:2400–2418.

- 419 Castro Morales, F., Gamerman, D., and Paez, M.S. (2013). State space models with spatial deformation.
420 *M.S. Environ Ecol Stat*, 20:191–214.
- 421 Costa, M. and Monteiro, M. (2015). Dynamic linear modeling of homogenized monthly temperature in
422 Lisbon. In Daniels, J. A., editor, *Advances in Environmental Research*, pages 203–215. Nova Science
423 Publishers.
- 424 Costa, M. and Monteiro, M. (2016). Bias-correction of Kalman filter estimators associated to a linear state
425 space model with estimated parameters. *J Stat Plan Infer*, 176:22–32. doi: 10.1016/j.jspi.2016.04.002.
- 426 Cunha, M., Gamerman, D., Fuentes, M., and Paez, M. (2017). A non-stationary spatial model for temper-
427 ature interpolation applied to the state of Rio de Janeiro. *J Roy Stat Soc C-App*, 66:919–939.
- 428 EEA (2018). European Environment Agency (2018). Global and European tempera-
429 tures. Available as a website at [https://www.eea.europa.eu/data-and-maps/indicators/
430 global-and-european-temperature-8/assessment](https://www.eea.europa.eu/data-and-maps/indicators/global-and-european-temperature-8/assessment).
- 431 Espírito Santo, F., Lima, I., Ramos, A., and Trigo, R. (2014). Trends in seasonal surface air temperature
432 in mainland Portugal, since 1941. *International Journal of Climatology*, 34:1814–1837.
- 433 Fischer, M. (2015). Predictable components in australian daily temperature data. *Journal of Climate*,
434 28:5969–5984.
- 435 Freitas, C., Dedekind, M., and Brill, B. (2015). A reanalysis of long-term surface air temperature trends in
436 New Zealand. *Environmental Modeling & Assessment*, 20:399–410. doi: 10.1007/s12665-015-5139-3.
- 437 Gardner, W., Napolitano, A., and Paura, L. (2006). Cyclostationary: half a century of research. *Signal*
438 *Process*, 86:639–697.
- 439 Harvey, A. (1996). *Forecasting structural time series models and the Kalman filter*. Cambridge University
440 Press.

441 Kleiber, W., Katz, R., and Rajagopalan, B. (2013). Daily minimum and maximum temperature simulation
442 over complex terrain. *Annals of Applied Statistics*, 7:588–612.

443 Kokic, P., Crimp, S., and Howden, M. (2011). Forecasting climate variables using a mixed-effect state-space
444 model. *Environmetrics*, 22:409–419. doi: 10.1002/env.1074.

445 Liu, G., Shao, Q., Lund, R., and Woody, J. (2016). Testing for seasonal means in time series data. *Envi-*
446 *ronmetrics*, 27:198–211. doi: 10.1002/env.2383.

447 Miranda, P., Coelho, F.E.S., Tomé, A.R., Valente, M.A., Carvalho, A., Pires, C., Pires, H.O., Pires, V.C.,
448 and Ramalho, C. (2002). 20th century portuguese climate and climate scenarios. In FD, S., K, F., and R,
449 M., editors, *Climate Change in Portugal: Scenarios, Impacts and Adaptation Measures (SIAM Project)*,
450 pages 23–83. Gradiva.

451 Monteiro, M., Pereira, I., and Scotto, M. (2010). Integer-valued autoregressive processes with periodic
452 structure. *J Stat Plan Infer*, 140:1529–1541.

453 Moreno, E., Girn, J., and Garc´ia Ferrer, A. (2013). A consistent on-line Bayesian procedure for detecting
454 change points. *Environmetrics*, 24:342–356. doi: 10.1002/env.2207.

455 Morosova, A. and Valente, M. (2012a). Homogenization of Portuguese long-term temperature data series:
456 Lisbon, Coimbra and Oporto. *Earth System Science Dat*, 4:187–213.

457 Morosova, A. and Valente, M. (2012b). Homogenization of Portuguese long-term temperature data series:
458 Lisbon, Coimbra and Oporto. PANGAEA. doi:10.1594/PANGAEA.785377.

459 Ngo, N. and Horton, R. (2016). Climate change and fetal health: The impacts of exposure to extreme
460 temperatures in New York City. *Environmental Research*, 144:158–164.

461 Obeysekera, J. and Salas, J. (1986). Modeling of aggregated hydrologic time series. *Journal of Hydrology*,
462 86:197–219.

- 463 Patterson, T., Thomas, L., Wilcox, C., Ovaskainen, O., and Matthiopoulos, J. (2008). State-space models
464 of individual animal movement. *Trends in Ecology & Evolution*, 33:87–94.
- 465 Perry, M. and Hollis, D. (2005). The development of a new set of long-term climate averages for the UK.
466 *International Journal of Climatology*, 25:1023–1039.
- 467 Poppick, A., McInerney, D.J., Moyer, E.J., and Stein, M.L. (2016). Temperatures in transient climates:
468 Improved methods for simulations with evolving temporal covariances. *Annals of Applied Statistics*,
469 10:477–505.
- 470 Ramos, A., Trigo, R.M., and Santos, F.E. (2011). Evolution of extreme temperatures over Portugal: and
471 future scenarios. *Climate Research*, 48:177–192.
- 472 Reich, B. (2012). Spatiotemporal quantile regression for detecting distributional changes in environmental
473 processes. *J Roy Stat Soc C-App*, 61:535–553.
- 474 Rodríguez, A. and Ruiz, E. (2012). Bootstrap prediction mean squared errors of unobserved states based
475 on the Kalman filter with estimated parameters. *Computational Statistics and Data Analysis*, 56:62–74.
- 476 Shumway, R.H. and Stoffer, D. (2017). *Time Series Analysis and Its Applications With R Examples*. Springer,
477 New York, 4th edition edition.
- 478 Smyth, G. (1996). Partitioned algorithms for maximum likelihood and other non-linear estimation. *Statistics*
479 *and Computing*, 6:201–216.
- 480 Tandeo, P., Ailliot, P., and Autret, E. (2011). Linear gaussian state-space model with irregular sampling:
481 application to sea surface temperature. *Stochastic Environmental Research and Risk Assessment*, 25:793–
482 804.
- 483 Trevin, B. (2013). A daily homogenized temperature data set for Australia. *International Journal of*
484 *Climatology*, 33:1510–1529.

- 485 Trigo, R. and Palutikof, J. (1999). Simulation of daily temperature for climate change scenarios over
486 Portugal: a neural network model approach. *Climate Research*, 13:45–59.
- 487 UN (2016). United Nations. <http://www.un.org/sustainabledevelopment/climate-change>. accessed in
488 December 7, 2017.
- 489 Ursu, E. and Perea, J. (2016). Application of periodic autoregressive process to the modeling of the Garonne
490 river flows. *Stochastic Environmental Research and Risk Assessment*, 30:1785–1795. doi: 10.1007/s00477-
491 015-1193-3.
- 492 Wang, W., Shao, Q., Yang, T., Peng, S., Yu, Z., Taylor, J., Xing, W., Zhao, C., and Sun, F. (2013).
493 Changes in daily temperature and precipitation extremes in the Yellow River basin, China. *Stochastic*
494 *Environmental Research and Risk Assessment*, 27:401–421.
- 495 William, C., Menne, M.J., and Thorne, P.W. (2012). Benchmarking the performance of pairwise homog-
496 enization of surface temperatures in the United States. *Journal of Geophysical Research*, 117. doi:
497 10.1029/2011JD016761.
- 498 Withers, C. and Nadarajah, S. (2015). Estimating trend from seasonal data: is daily, monthly or annual
499 data best? *Environmetrics*, 26:488–501. doi:10.1002/env.2356.
- 500 Xu, Y., Gao, X., Shi, Y., and Botao, Z. (2015). Detection and attribution analysis of annual mean temper-
501 ature changes in China. *Climate Research*, 63:61–71.

Table 1: Geodesic coordinates of three stations in Lisbon, Oporto and Coimbra

Station	Latitude	Longitude	Altitude
Lisbon	38° 43' N	9° 09' W	77 m
Porto	41° 08' N	8° 36' W	93 m
Coimbra	40° 12' N	8° 25' W	141 m

Table 2: Coefficients of determination and the log-likelihood of PMLSS models of Lisbon, Coimbra and Oporto.

	Lisbon	Coimbra	Porto
r^2	0.937	0.922	0.919
$-\log(\mathcal{L})$	2744.35	2795.64	2152.73

Table 3: Estimates of the mean rise of temperature Celsius degree per century, in Lisbon, Coimbra and Oporto.

	Lisbon	Coimbra	Porto
Jan	0.918	0.596	1.076
Feb	0.615	0.411	2.427
Mar	1.066	1.024	3.939
Apr	0.574	0.232	2.801
May	0.167	0.283	2.594
Jun	0.521	0.747	1.998
Jul	0.559	0.412	2.810
Aug	0.562	0.437	2.047
Sep	0.492	0.158	0.343
Oct	0.771	0.715	1.811
Nov	0.420	0.487	2.109
Dec	0.789	1.044	2.031
overall mean	0.621	0.545	2.166

Table 4: Estimates of the variances in the PMLSS models of Lisbon, Coimbra and Oporto.

	month	Lisbon	Coimbra	Porto
$\hat{\sigma}_{\varepsilon,s}^2$	Jan	0.404	0.488	0.330
	Feb	0.662	1.073	0.909
	Mar	0.457	1.061	0.749
	Apr	0.554	1.082	0.661
	May	0.751	1.174	0.633
	Jun	0.592	1.017	0.394
	Jul	0.438	0.782	0.475
	Aug	0.345	0.491	0.295
	Sep	0.582	1.077	0.658
	Oct	0.603	1.398	1.029
	Nov	0.305	0.836	0.720
	Dec	0.795	0.920	0.871
$\hat{\sigma}_{\omega}^2$		9.013×10^{-10}	9.992×10^{-12}	6.694×10^{-10}
$\hat{\sigma}_e^2$		0.548	0.562	0.643

Table 5: Estimates of autoregressive parameters in the PMLSS models of Lisbon, Coimbra and Oporto.

	month	Lisbon	Coimbra	Porto
$\widehat{\phi}_s$	Jan	0.549	0.914	0.428
	Feb	1.231	2.162	3.029
	Mar	2.703	2.376	1.265
	Apr	1.369	0.961	0.907
	May	0.537	0.402	1.165
	Jun	1.763	1.729	0.755
	Jul	0.566	0.232	1.326
	Aug	1.078	1.485	0.712
	Sep	0.221	0.035	0.227
	Oct	4.176	7.668	2.398
	Nov	1.011	4.142	1.231
	Dec	0.596	0.730	1.087
$\prod_{s=1}^{12} \widehat{\phi}_s$		0.804	0.869	0.900
$\widehat{\phi}_a$		0.381	0.307	0.351